

The Geomorphology of an Aleutian Volcano following a Major Eruption: the 7–8 August 2008 Eruption of Kasatochi Volcano, Alaska, and Its Aftermath

Authors: Waythomas, Christopher F., Scott, William E., and Nye, Christopher J.

Source: Arctic, Antarctic, and Alpine Research, 42(3) : 260-275

Published By: Institute of Arctic and Alpine Research (INSTAAR), University of Colorado

URL: <https://doi.org/10.1657/1938-4246-42.3.260>

BioOne Complete (complete.BioOne.org) is a full-text database of 200 subscribed and open-access titles in the biological, ecological, and environmental sciences published by nonprofit societies, associations, museums, institutions, and presses.

Your use of this PDF, the BioOne Complete website, and all posted and associated content indicates your acceptance of BioOne's Terms of Use, available at www.bioone.org/terms-of-use.

Usage of BioOne Complete content is strictly limited to personal, educational, and non - commercial use. Commercial inquiries or rights and permissions requests should be directed to the individual publisher as copyright holder.

BioOne sees sustainable scholarly publishing as an inherently collaborative enterprise connecting authors, nonprofit publishers, academic institutions, research libraries, and research funders in the common goal of maximizing access to critical research.

The Geomorphology of an Aleutian Volcano following a Major Eruption: the 7–8 August 2008 Eruption of Kasatochi Volcano, Alaska, and Its Aftermath

Christopher F. Waythomas*

William E. Scott† and

Christopher J. Nye‡

*Corresponding author: U.S. Geological Survey, Alaska Volcano Observatory, 4210 University Drive, Anchorage, Alaska 99508, U.S.A.
chris@usgs.gov

†U.S. Geological Survey, Cascades Volcano Observatory, 1300 SE Cardinal Court, Building 10, Suite 100, Vancouver, Washington 98683, U.S.A.
wescott@usgs.gov

‡State of Alaska, Division of Geological and Geophysical Surveys and Alaska Volcano Observatory, 3354 College Road, Fairbanks, Alaska 99709, U.S.A.
cnye@gi.alaska.edu

Abstract

Analysis of satellite images of Kasatochi volcano and field studies in 2008 and 2009 have shown that within about one year of the 7–8 August 2008 eruption, significant geomorphic changes associated with surface and coastal erosion have occurred. Gully erosion has removed 300,000 to 600,000 m³ of mostly fine-grained volcanic sediment from the flanks of the volcano and much of this has reached the ocean. Sediment yield estimates from two representative drainage basins on the south and west flanks of the volcano, with drainage areas of 0.7 and 0.5 km², are about 10⁴ m³ km⁻² yr⁻¹ and are comparable to sediment yields documented at other volcanoes affected by recent eruptive activity. Estimates of the retreat of coastal cliffs also made from analysis of satellite images indicate average annual erosion rates of 80 to 140 m yr⁻¹. If such rates persist it could take 3–5 years for wave erosion to reach the pre-eruption coastline, which was extended seaward about 400 m by the accumulation of erupted volcanic material. As of 13 September 2009, the date of the most recent satellite image of the island, the total volume of material eroded by wave action was about 10⁶ m³. We did not investigate the distribution of volcanic sediment in the near shore ocean around Kasatochi Island, but it appears that erosion and sediment dispersal in the nearshore environment will be greatest during large storms when the combination of high waves and rainfall runoff are most likely to coincide.

DOI: 10.1657/1938-4246-42.3.260

Introduction

Major volcanic eruptions have the capacity to radically transform landscapes by fundamentally altering the surface conditions that control the movement of water and sediment, the destruction and reestablishment of vegetation, and the type and character of plant and animal communities. The production of large quantities of volcanoclastic sediment during eruptive activity typically has profound and long-lasting effects on the surface hydrology and geomorphology of volcanoes, and many volcanically disturbed watersheds take decades to centuries to recover to pre-eruption conditions (Segerstrom, 1960, 1966; Shimokawa and Taniguchi, 1983; Chinen and Kadomura, 1986; Shimokawa et al., 1996; Suwa and Yamakashi, 1999; Major et al., 2000; Hayes et al., 2002; Major, 2004; Major and Yamakoshi, 2005; Gran and Montgomery, 2005; Dale et al., 2005; Major and Mark, 2006). Sediment yields from volcanoes that have recently erupted are among the highest known worldwide (Milliman and Syvitski, 1992; Walling and Webb, 1996; Major et al., 2000; Lavigne, 2004), and eruptions at island arc volcanoes are responsible for generating the bulk of the sediment on the seafloor in these areas (Kuenzi et al., 1979; Manville et al., 2009). Thus, most erupting stratovolcanoes are prodigious producers of sediment and at the drainage basin scale this sediment can have significant geomorphic and ecologic consequences.

Most stratovolcanoes have high relief and steep slopes, and incision and erosion of volcanic deposits following a large eruption is typically rapid because there is little to retard the erosive effects of flowing water (Swanson et al., 1983; Collins and Dunne, 1986; Swanson and Major, 2005). Rill and gully erosion are important post-eruption geomorphic processes that can

mobilize substantial amounts of sediment and introduce it to areas downslope. The redistribution of sediment on volcanoes may create a disturbance environment that persists for years to decades.

Kasatochi volcano in the Aleutian Islands of Alaska (Fig. 1) erupted on 7–8 August 2008 and radically altered the character of Kasatochi Island (Waythomas et al., 2010). Kasatochi has been a long-term biological study site of the U.S. Fish and Wildlife Service, which has deployed scientists to the island for more than a decade to monitor seabirds and marine life (Williams et al., 2010 [this issue]). A thorough investigation of the geology and eruptive history of Kasatochi was not part of those studies, and no geologists had ever visited the island for more than a few hours prior to the August 2008 eruption. The Kasatochi eruption completely destroyed nearly all preexisting terrestrial habitat and covered the flanks of the island and near-shore areas with a mantle of unconsolidated pyroclastic deposits ranging in thickness from less than one meter to tens of meters (Waythomas et al., 2010; Scott et al., 2010 [this issue]). The loss of habitat resulting from the eruption has raised important questions about the future significance of the island as a seabird-nesting site and how geomorphic changes on the island might affect both short- and long-term ecological recovery (Talbot et al., 2010 [this issue]; Williams et al., 2010 [this issue]; Jewett et al., 2010 [this issue]).

We conducted fieldwork in summer 2009 to systematically investigate the eruptive deposits and evaluate the primary geomorphic processes responsible for erosion and deposition of sediment both on the island and in the nearshore environment. In this paper, and in the paper by Scott et al. (2010 [this issue]), we also report our preliminary findings on geology and geomorphol-

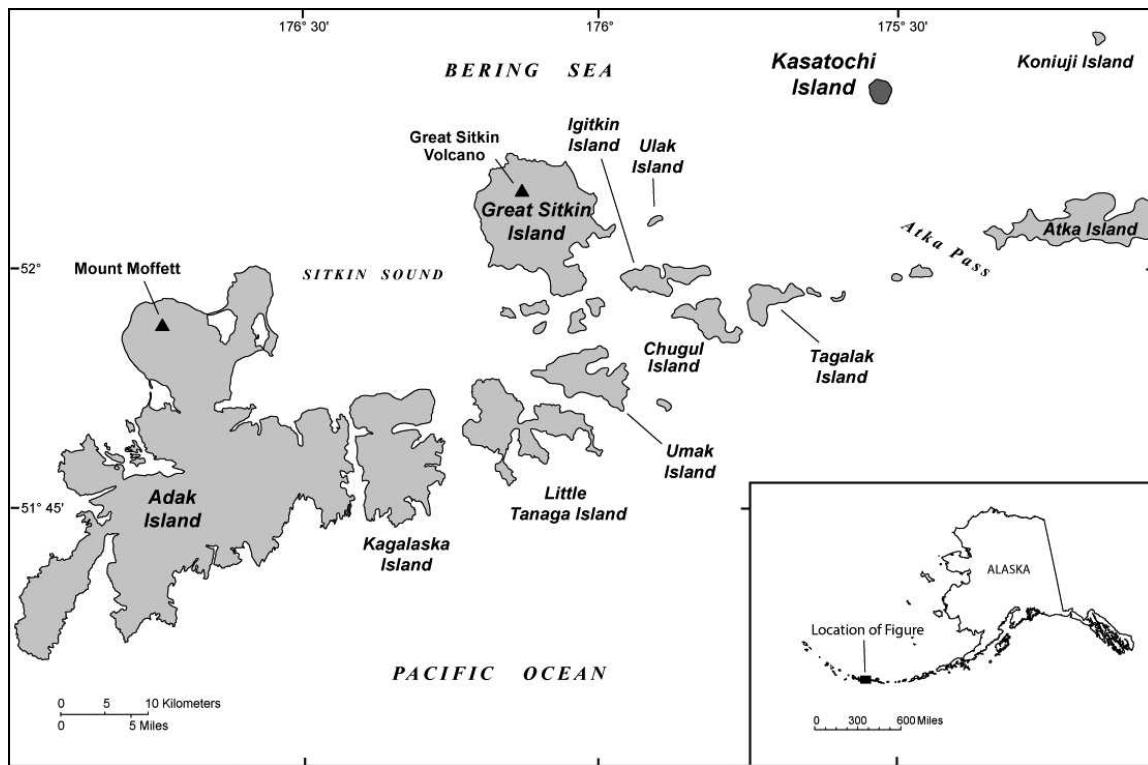


FIGURE 1. Location of Kasatochi Island in the west-central Aleutian Islands of Alaska.

ogy, and describe the implications of these results and the continued evolution of surficial features on the island and delivery of sediment to the sea.

Setting

GEOLOGY

Kasatochi volcano is the dominant landform of Kasatochi Island, an approximately 3 km diameter and approximately 314-m-high island in the central Aleutian Islands of Alaska (52.17°N latitude, 175.51°W longitude; Fig. 1). Prior to the 2008 eruption, vegetation on the volcano consisted of both maritime and alpine tundra, and included a variety of grasses, sedges, sphagnum mosses, lichens and forbs, but no trees or shrubs (Talbot et al., 2010 [this issue]). A circular, sharp-rimmed, steep-walled crater containing a brackish lake characterizes the summit of the volcano. There are no telemetered seismic instruments on the island, and the nearest seismic monitoring equipment is on Great Sitkin Island, about 35 km to the west, and on Atka Island, 90 km to the east.

Kasatochi Island is situated along the main east-west volcanic front of the central Aleutian Islands and is about 190 km north of the Aleutian Trench. Kasatochi Island lies in relatively shallow water (20–200 m) on the north side of a bathymetric feature called the Aleutian Ridge (Ryan and Scholl, 1989). Two noteworthy earthquakes have occurred within 50 km of Kasatochi Island, in 1957 ($M_w = 9.1$) (Sykes, 1971) and in 1986 ($M_w = 8.0$) (Engdahl et al., 1989). Kasatochi is surrounded by ocean and is thus vulnerable to tsunamis, although it is unknown if any of the documented historical tsunamis in the area have struck the island (Lander, 1996).

Pyroclastic deposits and lava flows that pre-date the 2008 deposits are exposed in sea cliffs and in the upper walls of the summit crater. Although these deposits have not been studied in

detail, they are primarily scoriaceous and pumiceous pyroclastic-flow deposits locally rich in lithic material derived from older lava flows inside the crater. The lava flows that make up the Kasatochi cone are undated and range in composition from basalt to andesite (Waythomas et al., 2010). The older unconsolidated deposits are indicative of an explosive eruptive history and evidence for possibly several significant eruptions within the past few thousand years. This indicates that the Kasatochi ecosystem has recovered from the effects of major volcanic disturbances in the past and that given sufficient repose time following the 2008 eruption, should recover again.

The 2008 eruption on 7–8 August was a large explosive (VEI 4) event that produced many pyroclastic flows that swept the island, tephra falls, many of which fell into the sea, and several ash and vapor clouds that were tracked by satellite for thousands of kilometers downwind of the volcano (Waythomas et al., 2010; Karagulian et al., 2010). The 7–8 August eruption lasted roughly 24 hours, and in that time the island was repeatedly swept by pyroclastic flows that deposited meters to tens of meters of unconsolidated volcanic sediment consisting of gravel, sand, silt, and boulders. The pyroclastic flows overran all flanks of the volcano and transported pyroclastic debris into the sea. The accumulation of pyroclastic debris in the nearshore zone resulted in seaward extension of the entire coastline about 400 m and increased the diameter of the island by about 800 m. Field studies in summer 2009 indicated that the bulk of the eruptive products from the 2008 eruption are pyroclastic-flow deposits, produced mainly by phreatomagmatic activity, that contain mostly accidental lithic debris derived from preexisting lava flows in the crater. The juvenile material in these deposits is pumiceous andesite (58–59% SiO_2) and it accounts for about 20–50% by volume of the deposits we examined (Waythomas et al., 2010).

As the eruption began to end, the eruptive style changed to a mode of nearly continuous ash emission and intermittent phreatic

TABLE 1
Monthly climate data for Adak, Alaska, 1949–2005. Data from Western Regional Climate Center.

	Jan	Feb	Mar	Apr	May	Jun	Jul	Aug	Sep	Oct	Nov	Dec	Annual
Average max. temperature (°C)	2.89	2.78	3.67	5.17	7.28	9.50	12.22	13.22	11.28	8.28	5.22	3.33	7.06
Average min. temperature (°C)	-1.72	-1.94	-1.06	0.50	2.56	4.89	7.06	8.11	6.44	3.44	0.56	-1.17	2.33
Average total precipitation (cm)	15.93	11.61	13.79	10.64	9.80	7.85	7.16	10.72	14.68	16.66	18.87	18.49	156.21
Average total snowfall (cm)	45.97	46.74	51.05	25.40	3.81	0.00	0.00	0.00	0.25	3.81	26.42	49.02	252.48
Average snow depth (cm)	5.08	7.62	5.08	0.00	0.00	0.00	0.00	0.00	0.00	0.00	0.00	2.54	2.54
Highest total precipitation (cm)	44.0	23.4	30.5	25.8	40.9	23.8	15.5	24.2	28.7	31.8	32.8	35.0	230.2
Twenty-four-hour maximum precipitation (cm)	9.1	5.7	6.1	12.1	12.3	6.4	6.0	6.2	11.7	8.5	7.5	13.9	
Average hourly maximum precipitation (cm hr ⁻¹)	0.38	0.24	0.25	0.50	0.51	0.27	0.25	0.26	0.49	0.36	0.31	0.58	

and phreatomagmatic activity. This resulted in the accumulation of a uniform cover of medium gray-brown fine ash and pyroclastic-surge deposits over all flanks of the volcano. These deposits are 2–3 m thick and consist of silt, fine sand, and granules that are easily eroded by channelized water flows, and turn to sticky muck when wet.

CLIMATE

Kasatochi Island has a distinctly Aleutian maritime climate that is typically cool, windy, wet, and cloudy. The region is strongly influenced by the Aleutian Low, a major climatological low-pressure feature that is an important component of northern hemisphere atmospheric circulation (Overland et al., 1999; Trenberth, 1990). The position and strength of the Aleutian Low influences the tracks of storms across the North Pacific and exerts a major control on winter temperature variability over the Bering Sea (Rodionov et al., 2005; Rodionov et al., 2007). Major storms associated with strong Aleutian Lows can be powerful, and sustained winds in excess of 22 m s⁻¹ are common during such storms (Rodionov et al., 2005). Primary storm tracks are from west to east, although variations to this primary pattern can occur on time scales of weeks to years (Anderson and Gyakum, 1989). The Aleutian Low intensifies during winter when large powerful storms may develop several times each month (Rodionov et al., 2007).

Although no weather stations have been formally maintained on Kasatochi Island, weather data has been systematically collected on nearby Adak Island (80 km west of Kasatochi) since September 1949 (Table 1). These data indicate that most of the precipitation falls during the autumn and winter (roughly October–April), and that areas near sea level can be snow covered from October–May. Thus, the typical snow-free months, and approximate period when significant surface runoff is expected, are from May–October. During these months, rainfall intensity at Adak has occasionally exceeded 6 cm in 24 hours although this is uncommon (Table 1). A probabilistic plot of precipitation data indicates that long periods of sustained rainfall are rare on Adak and that amounts exceeding 1.3 cm in 24 hours have about a 10% or less probability of occurrence (Fig. 2). The maximum average hourly rainfall intensity (May–October) determined from the 24-hour totals given in Table 1 range from 0.25–0.51 cm hr⁻¹. These data suggest that rainfall amounts sufficient to generate overland flow that leads to rill and gully erosion on Kasatochi may occur infrequently and are likely to be short (a few hours at most) in duration.

At or below freezing temperatures can occur at sea level from about November to April and on Adak there are typically 100–200 consecutive days per year during which the temperature remains above freezing. The average minimum winter temperature (Dec., Jan., Feb.) is -1.6 °C and there is an average of 12 days annually

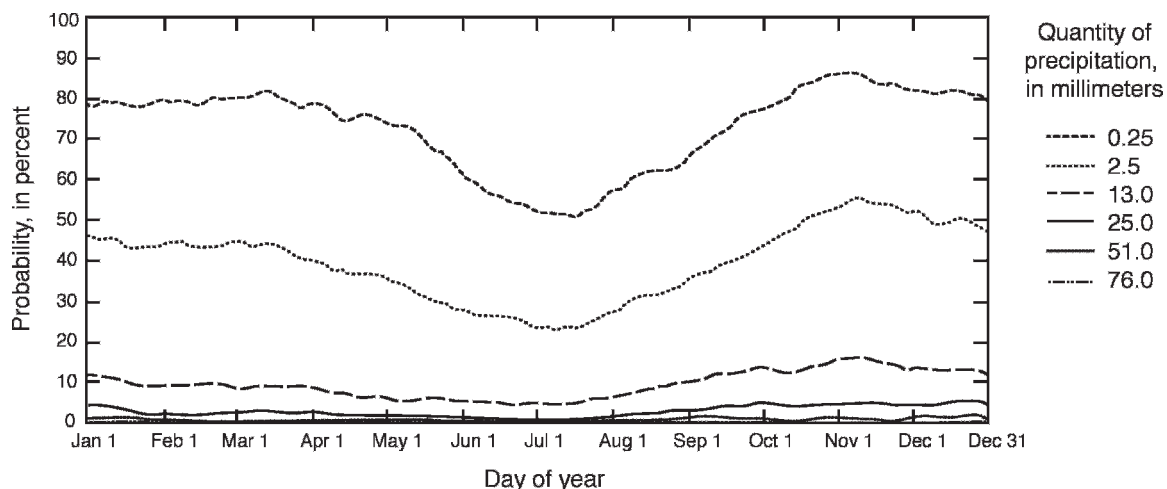


FIGURE 2. Probability of precipitation in a 1-day period, Adak, Alaska. These probabilities are likely broadly applicable to the general region and thus would generally apply to conditions on Kasatochi Island. Data from Western Regional Climate Center.

when the maximum temperature is ≤ 0 °C. It is possible that freeze-thaw processes play a role in mixing or disturbing near surface sediment, although this is not known. Permafrost does not occur in the region.

Surface Erosion and Watershed Processes

Surface erosion on the slopes of Kasatochi volcano controls the transfer of sediment to the marine environment and is largely a function of the local hydrologic conditions. Observations made during visits to the volcano in June and August 2009, and analysis of satellite images obtained on 17 Sept. 2008, 18 April 2009, and 13 Sept. 2009 indicated that extensive rill and gully erosion began shortly after the eruption and is continuing (Fig. 3). Before describing the gullies and extent of surface erosion on Kasatochi, some background on key gully-forming processes is presented to develop the conceptual framework for how and why these features originate and how they influence the surficial geology of the island.

A gully is a narrow, relatively deep, v-shaped or rectangular channel on a hillside formed by flowing water (Bull and Kirkby, 1997; Kirkby and Bracken, 2009). The flows that carve gullies are typically ephemeral and they are common in environments that have flashy hydrologic regimes (Erskine, 2005). A rill is similar to a gully but is smaller, on the order of centimeters to a few tens of centimeters in width. For the purposes of this study, we did not attempt to differentiate among rills and gullies, mainly because of the limitations imposed by the scale of the satellite images we used, which were about 1 m resolution. Thus, the data on surface erosion we present pertains to features whose width is ≥ 1 m.

Given sufficient rainfall, rill and gully networks can develop rapidly on sloping surfaces composed of relatively uniform grain size with no or little vegetation, such as the ash-covered flanks of a volcano. Once the gully network becomes established, the system evolves toward a quasi-stable channel system that adjusts to the pertinent boundary conditions, such as runoff, vegetation, and the physical characteristics of the channel bed and banks. Most gully systems are transport-limited because the supply of sediment exceeds the transport capacity of the flows within the gullies. Thus, until the gully reaches a quasi-equilibrium condition (i.e., typical flows no longer modify the channel in any significant way), transport, storage, and export of sediment from the drainage basin will continue. Here we focus on the growth of gullies and their role in eroding and redistributing the 2008 deposits, exhumation of the pre-eruptive surface, and the creation of coastal fans, as well as the export of sediment (or sediment yield) from the gully networks on Kasatochi Island to the marine environment.

Rill and gully development results from overland flow, and overland flow occurs when the rainfall rate exceeds the infiltration capacity. Infiltration capacity (I , expressed in mm hr^{-1}) refers to the ability of a surficial deposit to absorb water and is a key variable in determining the amount of surface runoff. Field experiments to determine the infiltration capacity of ash and pyroclastic-flow-mantled hillslopes following the 18 May 1980 eruption of Mount St. Helens found that post-eruption values for I were 2–5 mm hr^{-1} about four months after the eruption, and 4–7 mm hr^{-1} about one year after the eruption, well below pre-eruption estimates of 75–100 mm hr^{-1} for I in the same watershed of 75–100 mm hr^{-1} (Leavesley et al., 1989). Twenty years later, Major and Yamakoshi (2005) found that values for I had increased as much as ten times these post-eruption values but remained three to five times lower than pre-eruption values. Japanese scientists report values for I up to 35 mm hr^{-1} for

recently ash-covered slopes on Sakurajima, Usu, and Unzen Volcanoes (Shimokawa and Jitousono, 1987; Yamamoto, 1984). Although we did not measure I in the field on Kasatochi Island, we assume that values for I are similar to those reported in the literature. Infiltration capacity can be expressed as a relation among rainfall intensity (r), and surface runoff (R), such that $R = r - I$. If I is low or nearly zero, runoff will be proportional to rainfall intensity. We suspect that values for I on Kasatochi are low, because the apparent rainfall intensity determined from the Adak weather data is also low. Thus, most of what falls as rain runs off and does geomorphic work to form rills and gullies. This is typical of most hillslopes composed of fine volcanic ash (Collins and Dunne, 1986).

Overland flow exerts a shear force on the underlying substrate. When the shear force of the flow exceeds the shear resistance of the substrate, erosion will occur. Characterization of shear resistance (or detachment) in soils and surficial deposits has been a topic of much research because of the practical significance of soil erosion and the need to develop process-based soil erosion models (Wischmeier and Smith, 1978; Hairsine and Rose, 1992a, 1992b; Favis-Mortlock et al., 1998; Flanagan et al., 2001; Casali et al., 2003).

Overland flow is directed by surface irregularities and concentrates in small depressions thereby initiating rills, which may enlarge to gullies. Studies of natural gully development have shown that the initial phase of rill and gully formation is the most dynamic, and changes in gully geometry occur rapidly (Sidorchuck, 1999). Once the gully geometry becomes relatively stable, and significant changes in width, length, depth, area and volume only occur during large or extreme rainfall events, export of sediment from the gully system is largely controlled by erosion of the gully base and sediment transport along the floor of the gully. Increases in width of the gully base may lead to undercutting of the gully walls that may lead to collapse and overall gully widening. This stage of gully development is influenced by the particle size of the material that accumulates on the gully floor, or is left behind as a lag deposit. Cobble and larger size particles tend to armor the gully bed and inhibit deepening of the gully, but promote lateral erosion and undercutting.

A fundamental landscape property that describes the degree of dissection by gullies and stream channels is drainage density (Horton, 1945). Drainage density is the ratio of total channel length to drainage-basin area. Changes in drainage density with time indicate that the threshold for erosion by runoff has been exceeded during individual rainfall events, and that the drainage system has yet to reach a state of quasi-equilibrium where routine rainfall events no longer bring about appreciable changes in drainage density. Time-dependent changes in drainage density also are surrogate measures of erosion because an increase in channel length must reflect channel head processes such as landsliding or gullying (Montgomery and Dietrich, 1989). Eventually the rates of gully development will decline and drainage density will approach a steady-state value or perhaps decrease. This is commonly due to the stabilizing effects of vegetation growth (Collins and Bras, 2004; Istanbuluoglu and Bras, 2005). We note that prior to the 2008 eruption of Kasatochi, the flanks of the volcano were covered with a nearly continuous mantle of herbaceous tundra, and no surface streams or drainages were present. Thus, prior to the eruption, the drainage density was very low, if not zero, and over time, we expect that the island will return to this condition.

Removal of volcanoclastic sediment from the flanks of Kasatochi volcano by rill and gully erosion ultimately results in export of sediment to coastal fans or directly to the sea. The net export of sediment from a drainage basin is commonly expressed in



FIGURE 3. Typical gullies on the flanks of Kasatochi volcano. (A) Southeast flank of Kasatochi showing typical gully pattern. Arrow locates person for scale. (B) View looking down the axis of a v-shaped gully on the east flank of the volcano. Maximum gully depth here is about 3 m. Photographs by C. Waythomas, 12 June 2009.

terms of a volume per unit area per year and is known as sediment yield (Waythomas and Williams, 1988; Walling and Webb, 1996). Studies of erosion and export of sediment on active volcanoes indicate that sediment yield usually reaches maximum values within

months to a few years following an eruption (Swanson et al., 1983; Rosenfeld, 1987; Janda et al., 1996; Major et al., 2000; Lavigne, 2004) and then declines as channels stabilize and vegetation gets reestablished (Schumm and Rea, 1995; Major, 2004).

Initial landscape changes on Kasatochi Island were, and future changes will continue to be, mainly on hillslopes and shorelines. Assessments of these changes during the first year after the eruption are based on analysis of satellite images of Kasatochi Island, supplemented with measurements and field observations made during brief trips to the island in late August 2008 and in June and August 2009.

Gully length was measured using the commercial GIS software ArcMap from satellite images of Kasatochi Island obtained on 17 Sept. 2008, 18 April 2009, and 13 Sept. 2009. Stereo satellite images acquired on 18 April 2009 were used to generate a 5-m digital elevation model (DEM) and a derived topographic map of the island (Fig. 4). Two drainage basins were chosen for drainage network evaluation and are shown on Figure 5. Basin 1 is located on the south flank of the volcano and has a drainage area of 0.7 km². Basin 2 is located on the west flank of the island and has a drainage area of 0.5 km². In each drainage basin, gully length was measured in ArcMap and then summed to obtain total gully length for the three satellite image dates. Total gully length was then divided by drainage area to obtain drainage density (Table 2).

Total gully length from the two drainage basins also provides a way to estimate the amount of sediment removed by gully erosion using estimates of average cross-sectional area of gullies in the basins. Individual gully cross sections vary widely in size, from <1 m² to as large as a few tens of square meters, and are generally more v-shaped than box-shaped (Fig. 5). On the basis of our observations during summer 2009, we estimate average gully cross-sectional area is between 1 and 4 m², and our resulting volume estimates of sediment removed by gully erosion (Table 3) are probably accurate to at least an order of magnitude. These estimates are used to determine aerially averaged values for the amount of sediment removed by gully erosion for the entire island as a function of time, which we then extrapolate into the future based on power-law relations fit to the sediment loss data.

Field time on Kasatochi Island in summer 2009 was brief, and it was possible to measure gully cross sections in only a few locations (Fig. 5). Four cross sections were measured with a tape measure and tag line, on the east and west sides of the island. The coordinates of the cross-section endpoints were determined by handheld GPS and marked with permanent monuments.

The pyroclastic deposits generated by the 2008 eruption flowed into the sea and extended the Kasatochi coastline about 400 m seaward (Waythomas et al., 2010). Almost immediately after the eruption ended, wave erosion of the coastline began and new beaches began to form (Fig. 6). Most beaches grew by landward retreat of coastal cliffs, but in some areas on the southern end of the island, beaches accreted as a result of longshore drift delivering sediment to the south. Changes in beach width are apparent in satellite imagery and show distinct changes over the approximately one-year period since the eruption ended. Beach width was measured on the three satellite images for each sector of the island as indicated on Figure 4. Measurements were made normal to the coastline from the waterline to the base of wave cut cliffs that were evident in the satellite images, or to the contact between the accreting beach and the 2008 deposits. In most sectors, these measurements provide an estimate of the amount of beach cliff retreat caused by wave erosion of the deposits emplaced during the 2008 eruption (Fig. 7). The areal extent of beach erosion also was mapped on the 13 September 2009 satellite image and used to estimate the volume of sediment eroded by wave action.

Analysis of satellite images obtained before and after the August 2008 eruption shows distinct changes in the morphology of the island, surface erosion, evolution of the drainage networks and amount of coastal erosion (Tables 4 and 5). Of greatest significance is the increase in planimetric area of the island from 5.03 km² to 7 km² (about a 40% increase) and an increase in diameter of about 800 m. Progradation of the coast was a direct result of the generation of pyroclastic flows during the eruption which produced fans and sheets of debris that accumulated on the shallow seafloor surrounding Kasatochi Island. As the eruption progressed, unconsolidated, clastic volcanic debris and ash was deposited over the entire island and formed deposits ranging from <1 m to 10–20 m thick (Waythomas et al., 2010; Scott et al., 2010 [this issue]). During the waning stages of the eruption, fine-grained ash and pyroclastic-surge deposits accumulated on the flanks of the volcano and formed a uniform surface mantle that was soon modified by fluvial erosion as rills and gullies developed during rainfall events. We document evolution of the drainage network by an increase in drainage density in both of the basins (Table 2; Fig. 8). Power-law relations have been fit to these data to extrapolate into the future to estimate how the drainage density could evolve over the next 5–10 years. It is uncertain if changes in drainage density over time will follow these preliminary trends, or level off and show little or no change beyond what has already occurred. At Mount St. Helens, annual sediment yields leveled off by about 5 years after the 1980 eruption, but this area receives considerably more rainfall than does the Kasatochi region. It is also worth noting that a single large storm could generate a more evolved drainage network that would be little modified thereafter by typical runoff producing rainstorms. Likewise, a prolonged period of less-than-normal precipitation could delay continued evolution of the drainage network. If hydrologic conditions do not change significantly from the first year after the eruption, it is possible for changes in drainage density to follow the empirically derived trends, but for how long is not known.

The evolution of the drainage network also reflects the net erosion of surficial sediment from the flanks of the volcano. An estimate of the amount of erosion and sediment yield for the two drainage basins evaluated was calculated from estimates of average gully width, depth, and total length (Table 3). Two estimates are given for basins 1 and 2 and are based on values for width and depth of one and two meters to obtain a minimum and maximum estimate. An approximation of sediment yield for the year following the eruption was derived from analysis of the satellite image acquired on 13 September 2009 using the method described above. The sediment yield of basin 1 ranges from 30 to $120 \times 10^3 \text{ m}^3 \text{ km}^{-2} \text{ yr}^{-1}$ and $17\text{--}69 \times 10^3 \text{ m}^3 \text{ km}^{-2} \text{ yr}^{-1}$ for basin 2. These values are comparable to those observed in other volcanic watersheds affected by recent eruptive activity (Fig. 9).

Estimates of the amount of sediment removed by gully erosion in basins 1 and 2 were used to calculate cumulative sediment volumes lost by erosion for the entire island (Fig. 10). For basins 1 and 2, maximum sediment loss estimates in m³ per km² were calculated (Table 3) and then extrapolated over the total area of the island covered by erodible volcanic deposits (about 5.5 km²). These estimates were plotted versus time since the eruption and power-law equations were fit to these data yielding relations expressing the cumulative maximum sediment volume removed by erosion as a function of time since the eruption using the data from the two study basins.

The extrapolation of the power-law curves assumes that evolution of the drainage network will continue over the next 5–

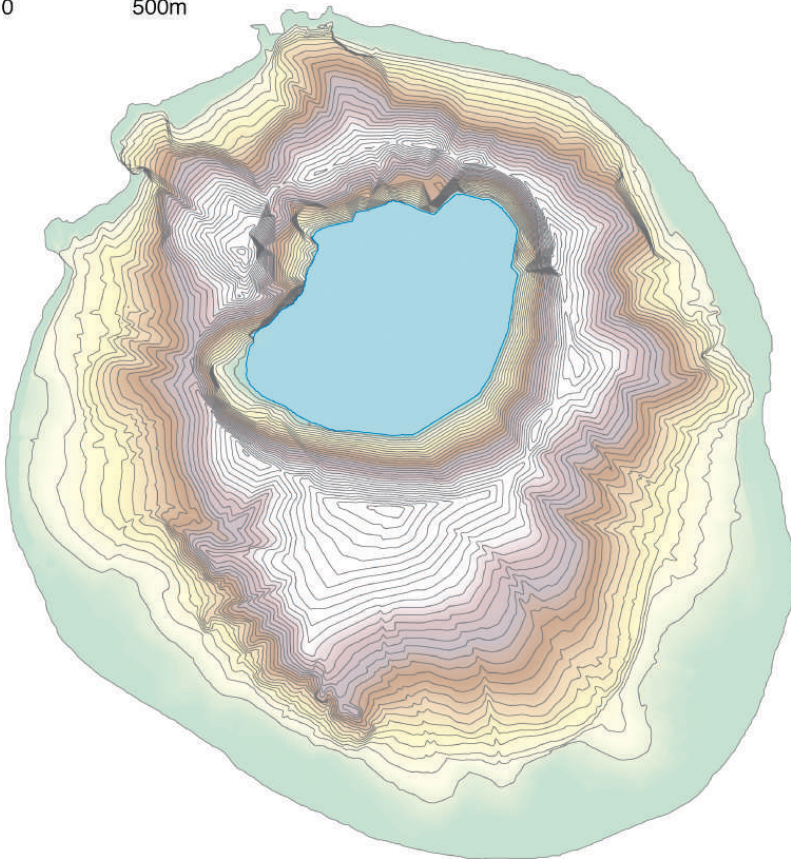
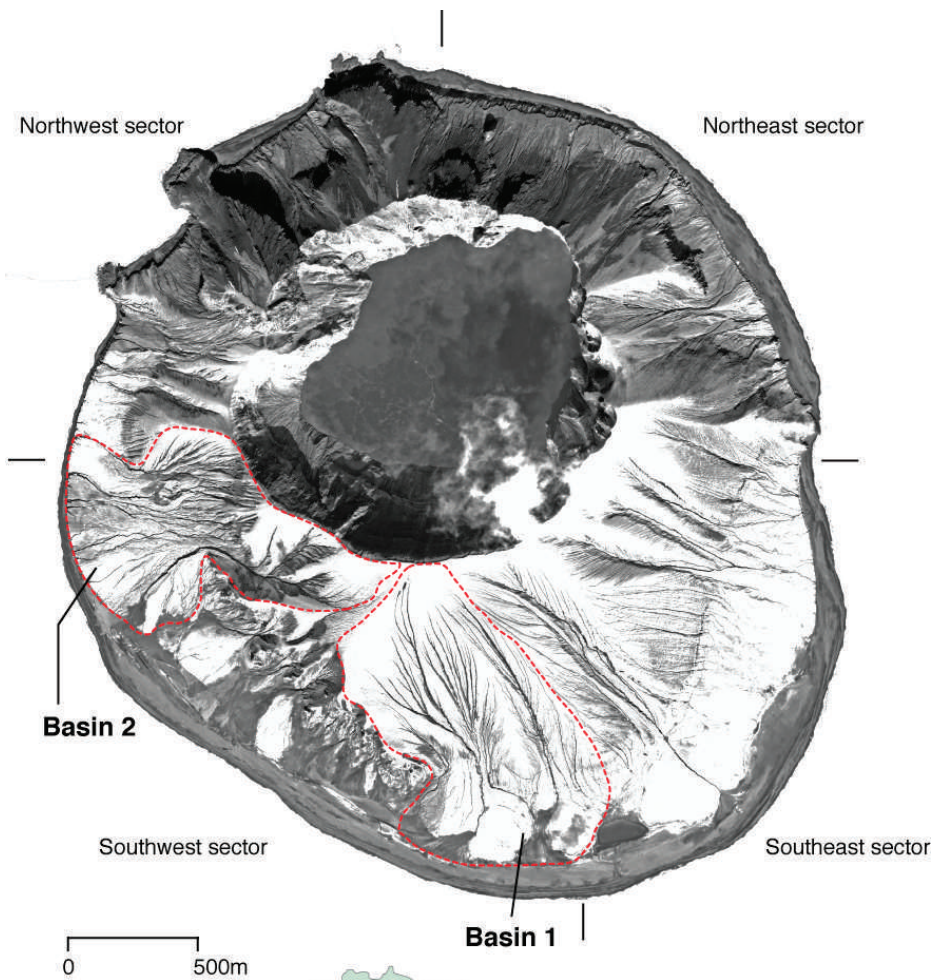


FIGURE 4. Quickbird satellite image and digital elevation model of Kasatochi Island, 18 April 2009. Drainage basins 1 and 2 indicated by red dashed lines. Basin 1 has a drainage area of 0.72 km², and basin 2 has a drainage area of 0.52 km². The contour interval of the DEM is 10 meters and the blue contour inside the crater is -10 meters.

TABLE 2

Drainage basin area and gully length data as determined from Quickbird satellite images acquired on 17 September 2008, 18 April 2009, and 13 September 2009.

		17 Sept. 2008	18 April 2009	13 Sept. 2009
Basin 1	Total gully length (km)	4.3	15.1	21.7
	Drainage area (km ²)	0.7	0.7	0.7
	Drainage density (km ⁻¹)	5.9	20.8	30.0
Basin 2	Total gully length (km)	3.0	8.7	8.9
	Drainage area (km ²)	0.5	0.5	0.5
	Drainage density (km ⁻¹)	5.7	16.8	17.2

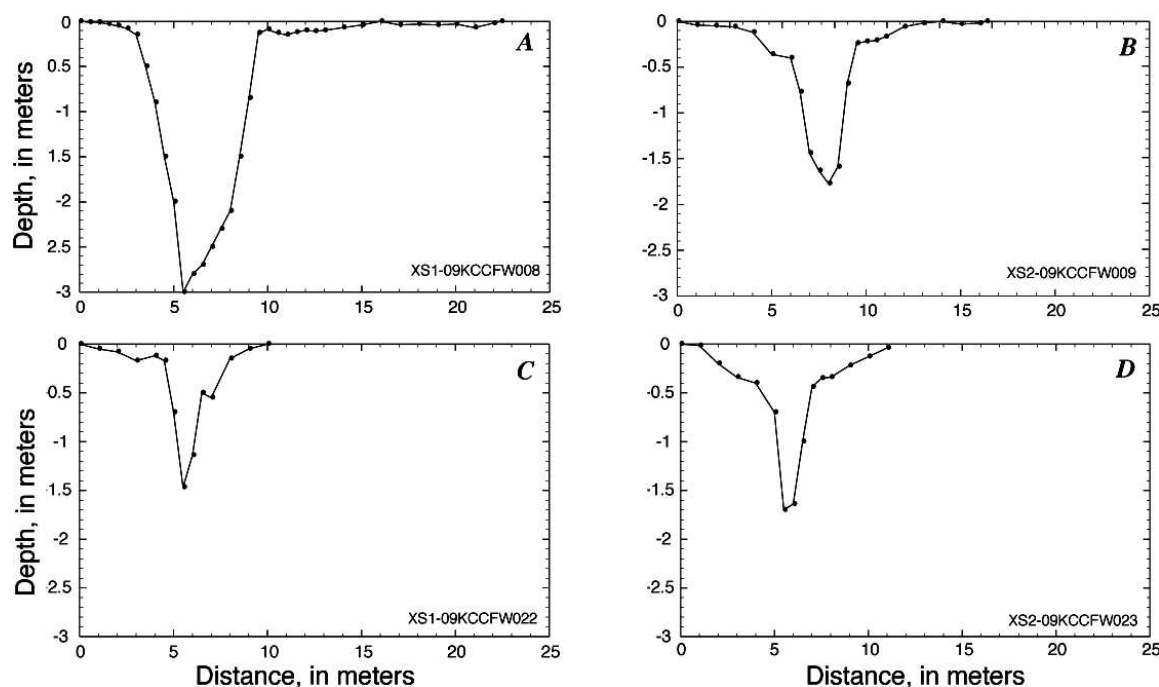


FIGURE 5. Gully cross sections from two locations on Kasatochi Island. Cross sections A and B are located on the east flank, cross sections C and D are located on the west flank.

10 years and sediment production will follow power-law relations similar to those derived above. The projected trends are inconclusive as they show almost linear and exponential changes over time. Other erosion studies on volcanoes affected by thick ash fall have shown that after an initial period of high sediment yield; the amount of erosion will level off and decline as the landscape begins to stabilize (Collins and Dunne, 1986; Major et al., 2000). This occurred over a period of 3–5 years at Mount St. Helens

following the 1980 eruption (Collins and Dunne, 1986; Major et al., 2000). As of 13 September 2009, the estimated total amount of sediment removed by gully erosion on Kasatochi was between 3.8×10^5 and 6.6×10^5 m³.

Erosion of the coastline by waves is also a mechanism for geomorphic change on the island and introducing sediment into the sea. After the eruption ended, pyroclastic-flow, surge, and fall deposits extended into the ocean, but were soon eroded back to

TABLE 3

Sediment loss and sediment yield estimates for drainage basins 1 and 2.

		17 Sept. 2008	18 April 2009	13 Sept. 2009
Basin 1	Minimum* sediment volume lost (m ³)	4300	15,006	21,700
	Maximum† sediment volume lost (m ³)	17,200	60,240	86,800
	Drainage area (km ²)	0.7	0.7	0.7
	Sediment yield (m ³ km ⁻² yr ⁻¹)			30–120 × 10 ³
Basin 2	Minimum* sediment volume lost (m ³)	2970	8750	8940
	Maximum† sediment volume lost (m ³)	11,880	35,000	35,760
	Drainage area (km ²)	0.5	0.5	0.5
	Sediment yield (m ³ km ⁻² yr ⁻¹)			17–69 × 10 ³

* Minimum sediment volume lost calculated as total gully length × width × depth, where width = 1 m, and depth = 1 m.

† Maximum sediment volume lost calculated as total gully length × width × depth, where width = 2 m, and depth = 2 m.



FIGURE 6. Coastline along the east side of Kasatochi Island, 22 August 2008, about 2 weeks after the eruption. The beach width at this time was about 2–3 meters, and the bluff on the left is about 1 m in height. The pyroclastic deposits exposed along the coastline are highly susceptible to wave erosion.

form new beaches (Fig. 6). Changes in beach width as determined from satellite images (Table 4) indicate the progressive erosion of the coastline by waves (Fig. 11). In the first few months or so after the eruption, wave action probably liberated significant amounts of sediment from the eroding coastline. As beach width increases over time, progressively larger waves will be required to cross widening beaches and reach exposed deposits, unless the outer beach face is also being eroded at a rate similar to retreating beach cliffs.

The preferred nesting habitats for seabirds on Kasatochi Island are talus accumulations and bedrock rubble along the coastline (Williams et al., 2010 [this issue]). The general extent of these areas prior to the 2008 eruption is shown on Figure 12. By 13 September 2009, areas of bedrock and a small patch of talus on the northwest coast that were covered by 2008 eruptive deposits had been exhumed by wave action (Fig. 12). The increase in beach width from 8 August 2008 to 13 September 2009 reflects retreat of wave-cut scarps inland as a function of wave erosion. The rate of

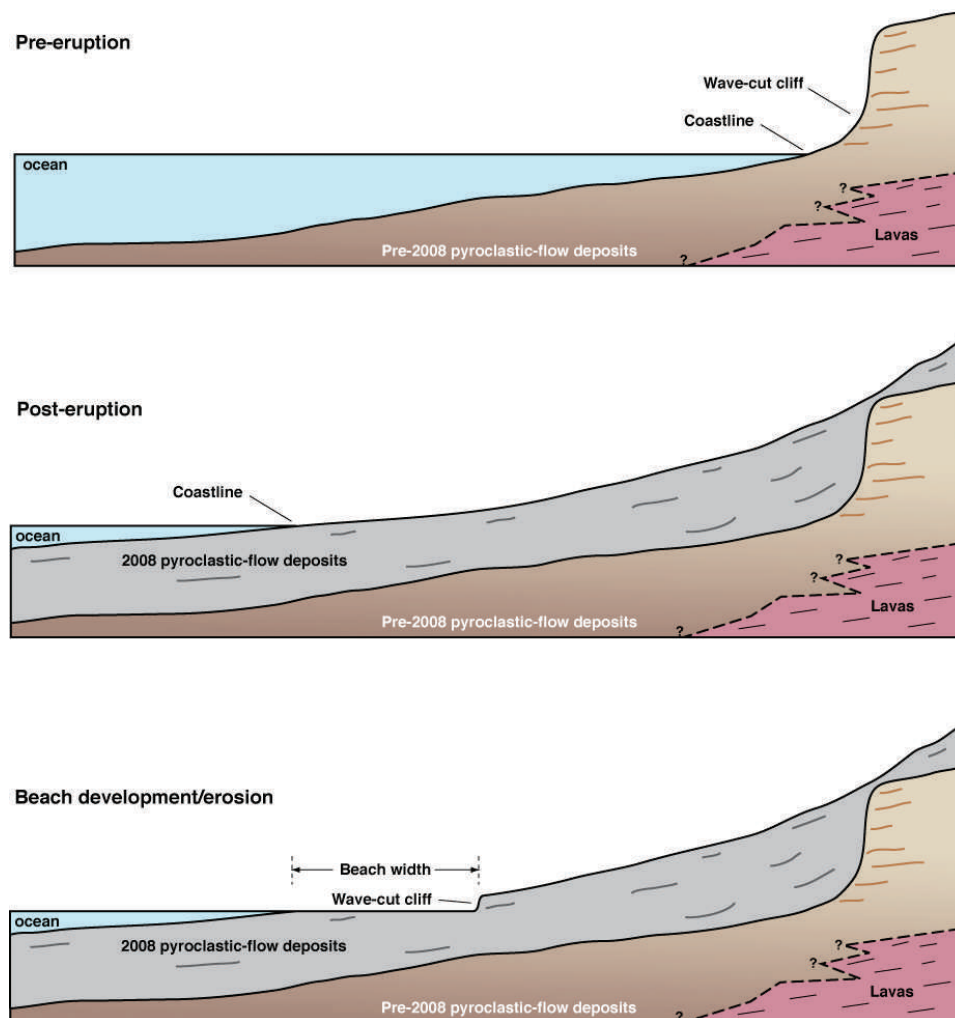


FIGURE 7. Generalized cross sections of the Kasatochi Island coastline showing pre- and post-eruption morphology. The 2008 eruption extended the coastline about 400 meters seaward, and soon after, wave action initiated beach erosion of the emplaced pyroclastic-flow deposits.

TABLE 4

Kasatochi Island beach width data. Beach width was measured as the distance from about the middle of the swash zone to the base of the wave cut cliff, or the point of onlap of beach deposits on eruptive deposits, normal to the coastline, as evident in satellite images. The island was divided into four equal quadrants to define the sectors.

	17 Sept. 2008	18 April 2009	13 Sept. 2009
NW Sector			
Maximum width (m)	55	122	142
Mean width (m)	36	66	91
Standard deviation	10	32	23
NE Sector			
Maximum width (m)	43	126	144
Mean width (m)	35	95	104
Standard deviation	6	22	27
SE Sector			
Maximum width (m)	141	201	239
Mean width (m)	51	138	145
Standard deviation	33	43	51
SW Sector			
Maximum width (m)	48	227	250
Mean width (m)	36	131	159
Standard deviation	6	62	52

erosion for this time period ranges from 0.22 to 0.39 m day⁻¹ and at this rate it would take 3–5 years for the coastline to retreat approximately 400 m to the position of the pre-eruption coastline. The total area of new beach generated by wave erosion as determined from the 13 September 2009 satellite image is about 8.78×10^5 m² and this corresponds to about 1.16×10^6 m³ of material removed by wave erosion assuming the average thickness of material eroded is about 2 m. The estimated total volume of sediment removed by gully erosion is somewhat less (between 3.8×10^5 and 6.6×10^5 m³). Thus, it appears that wave erosion has introduced more sediment into the marine environment than has rill and gully erosion.

The 2008 eruption of Kasatochi volcano also caused noteworthy changes in crater morphology. The perimeter of the pre-eruption crater was about 4.2 km, and after the eruption the crater perimeter increased to 4.8 km. The maximum width of the crater before the eruption was 1.26 km, and had increased to 1.5 km. The greatest change occurred on the southwest sector of the crater, where a large amount of the crater wall was removed and the rim was extended about 350 m. We infer that enlargement of the crater was the result of undercutting of the crater walls by explosions that led to foundering and collapse of rock debris into the erupting vent(s). This probably happened several times throughout the most energetic part of the eruption and was likely the mechanism that generated the bulk of the lithic-rich pyroclastic-flow deposits (Waythomas et al., 2010; Scott et al., 2010 [this issue]).

Discussion

Analysis of satellite images and field observations indicate that erosion of the ash and pyroclastic-flow mantled slopes of Kasatochi volcano is contributing mainly silt and sand sized sediment to the marine environment. We do not address the fate of this sediment in the sea. It is clear that runoff-induced erosion and wave action are the primary geomorphic processes associated with sediment production. Soon after the eruption ended, wave erosion of the coastline began, and rill and gully erosion on the slopes of the volcano commenced with the onset of rainfall events sufficient

to generate sustained overland flow. As the depth, velocity, shear stress, and stream power of overland flow increased, it exceeded the erosion threshold of the ash and pyroclastic mantle, and rills and gullies developed (Fig. 13). The initial period of gully formation and wave erosion of the coastline was likely the time of maximum sediment yield because the drainage network was rapidly developing on the virgin slopes of the volcano and the exposed coastline offered no buffer to advancing ocean waves (Fig. 13A). Thus, sediment directly reached the sea. As the drainage network evolved, gully widths increased and gully floors armored with coarse sediment; as a result sediment storage time in the gully network increased and delivery to the sea declined. Simultaneously, wave erosion of the coastline increased beach width and alluvial fans developed at the mouths of gullies (Fig. 13B). This provided another means of storing sediment on the island and decreasing the amount reaching the ocean. As beach width increases, more area is available for alluvial fan development, and more sediment will be retained within these fans (Fig. 13C). Eventually, gully development will stabilize and extension of existing gullies will only occur during extreme rainfall events.

Despite the susceptibility of the ash-covered hillslopes to erosion, regional weather data indicate that rainfall amounts and durations are typically low, and therefore major changes in the amount of gully erosion already evident are not expected. However, the behavior of the Aleutian Low and the nature of storm climatology in the region are variable, and it remains possible for severe storms to affect Kasatochi Island at almost any time. Large or extreme storms would cause additional erosion and drainage networks would likely extend, sediment would mobilize from gully systems, and significant coastal erosion would occur.

Significant amounts of coastal erosion have occurred since the 2008 eruption. Beach width data obtained from satellite images of Kasatochi Island (Table 6) indicate average rates of coastal erosion of 0.2–0.4 m day⁻¹ (80–140 m yr⁻¹). These are extreme rates of erosion, but given the nature of the environment at Kasatochi—a coastline extended into the sea by loose, unconsolidated pyroclastic deposits at an isolated unprotected island—such rates are not surprising. Over time the rates of coastline retreat will decline, but the island will always be vulnerable to wave erosion because of its location. It may be that the sediment contributed to the marine environment by wave action and surface erosion will eventually be released episodically, chiefly during extreme low frequency storms. To summarize these concepts, a conceptual temporal-geomorphic framework is presented in Figure 14.

Conclusions

Analysis of satellite images of Kasatochi volcano and field studies in 2009 have shown that within one year of the 7–8 August 2008 eruption some significant geomorphic changes associated with surface and coastal erosion have occurred. The primary cause of surface erosion is rainfall runoff, and rill and gully erosion on the flanks of the volcano have removed significant quantities of fine-grained volcanic sediment that has reached the ocean. Sediment yield from two drainage basins on the south and west flanks of the volcano are comparable to sediment yield estimates at other volcanoes and highlight the extreme susceptibility to erosion and sediment production that are characteristic of active volcanoes.

Studies of sediment yield at other active volcanoes indicate that peak sediment export at the drainage basin scale occurs within 2–3 years following a large eruption. Based on the erosion

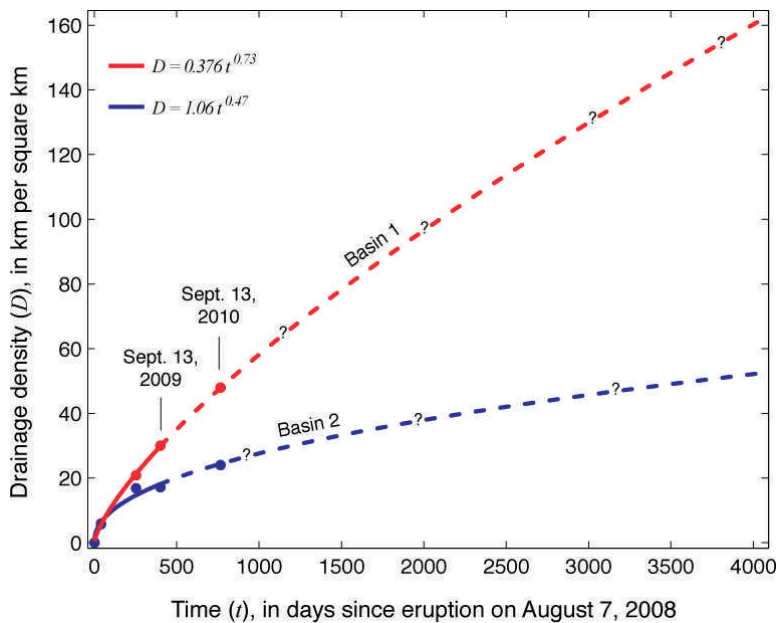


FIGURE 8. Drainage density versus time since the 7–8 August 2008 eruption for basins 1 and 2. Dashed lines show extrapolated trends based on power-law fits to drainage density data obtained from satellite images on 17 September 2008, 18 April 2008, and 13 September 2009.

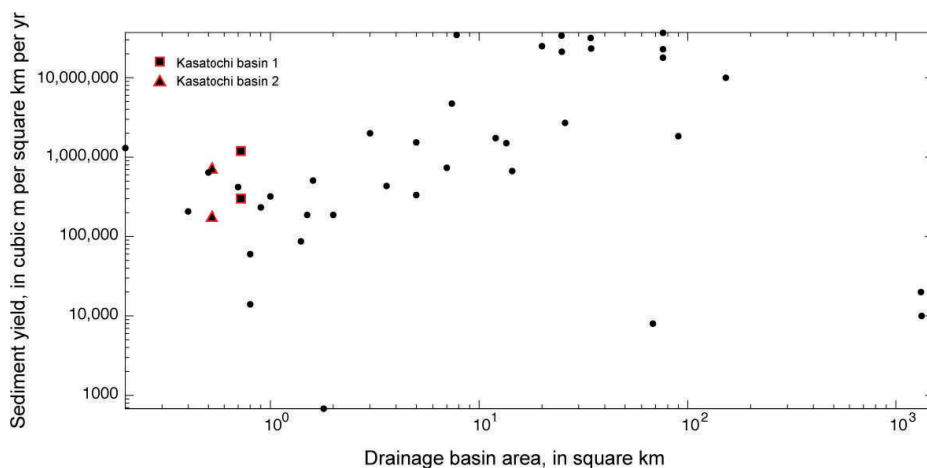


FIGURE 9. Sediment yield versus drainage basin area for drainages affected by volcanic eruptions worldwide (data from Lavigne, 2004). Also indicated are sediment yield estimates for the two drainage basins evaluated on Kasatochi Island, calculated using different values for cross-sectional area. This plot shows a general increase in sediment yield with increasing drainage basin area that is characteristic of watersheds on volcanoes affected by deposition of fragmental volcanic debris. No mathematical significance is implied because of the spurious nature of the relation among sediment yield and drainage basin area arising from a common unit in x and y .

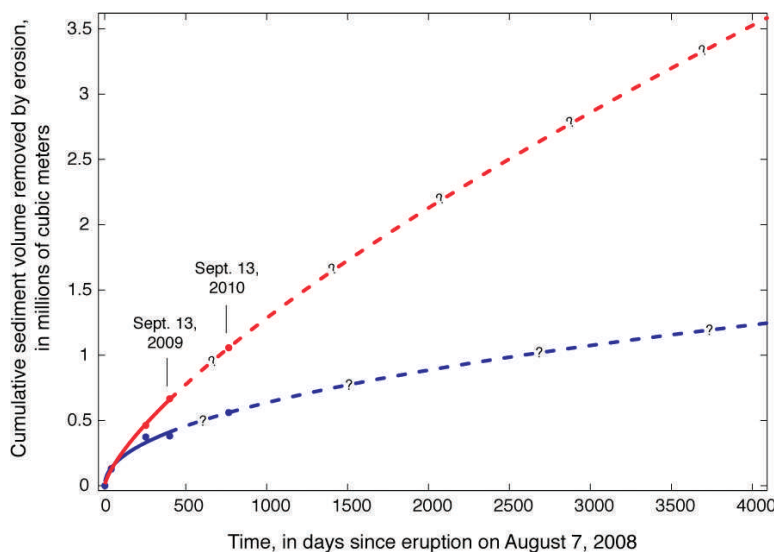


FIGURE 10. Cumulative sediment volume removed by gully erosion versus time since the 7–8 August 2008 eruption was determined by estimating the amount of sediment eroded from gullies in each of the two drainage basins evaluated for the three time periods for which we have satellite images. The maximum sediment loss estimates were recalculated in terms of a volume per square km and then multiplied by the area of the island (without the crater) to obtain estimates of cumulative sediment volume lost by erosion. It is uncertain if the amount of erosion will follow the power-law fits to this data over the next 5–10 years.

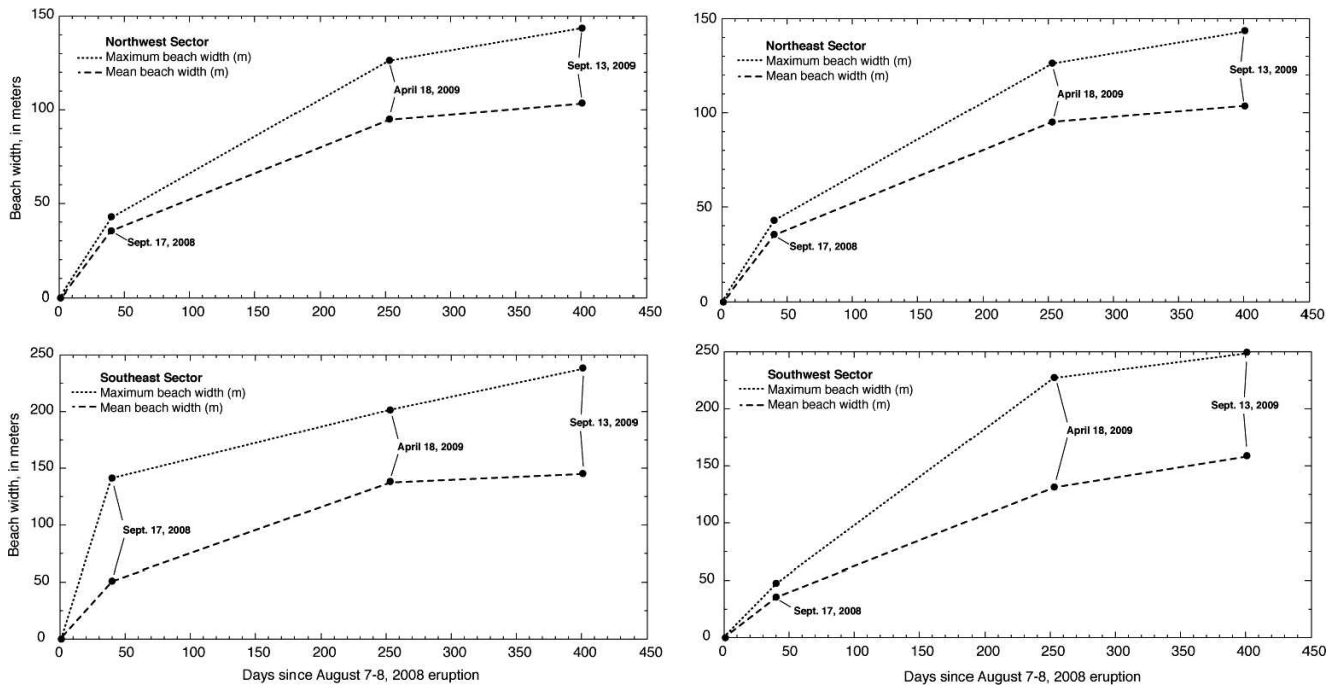


FIGURE 11. Changes in beach width versus time for each sector of Kasatochi Island. Sector designations shown on Figure 5. Beach width was measured on satellite images and is the distance from the water line to the emergent wave-cut cliff normal to the coastline.

data we obtained from our analysis of satellite images, it appears that gully lengthening is still occurring, but may be increasing at a slower rate than after the first six months or so following the 2008 eruption. However, it may be too soon to identify significant

trends in the erosion data, and the volcano remains very susceptible to further erosion and gully development because infiltration rates are probably still low, no significant vegetation has begun to emerge, and storms producing significant (for the

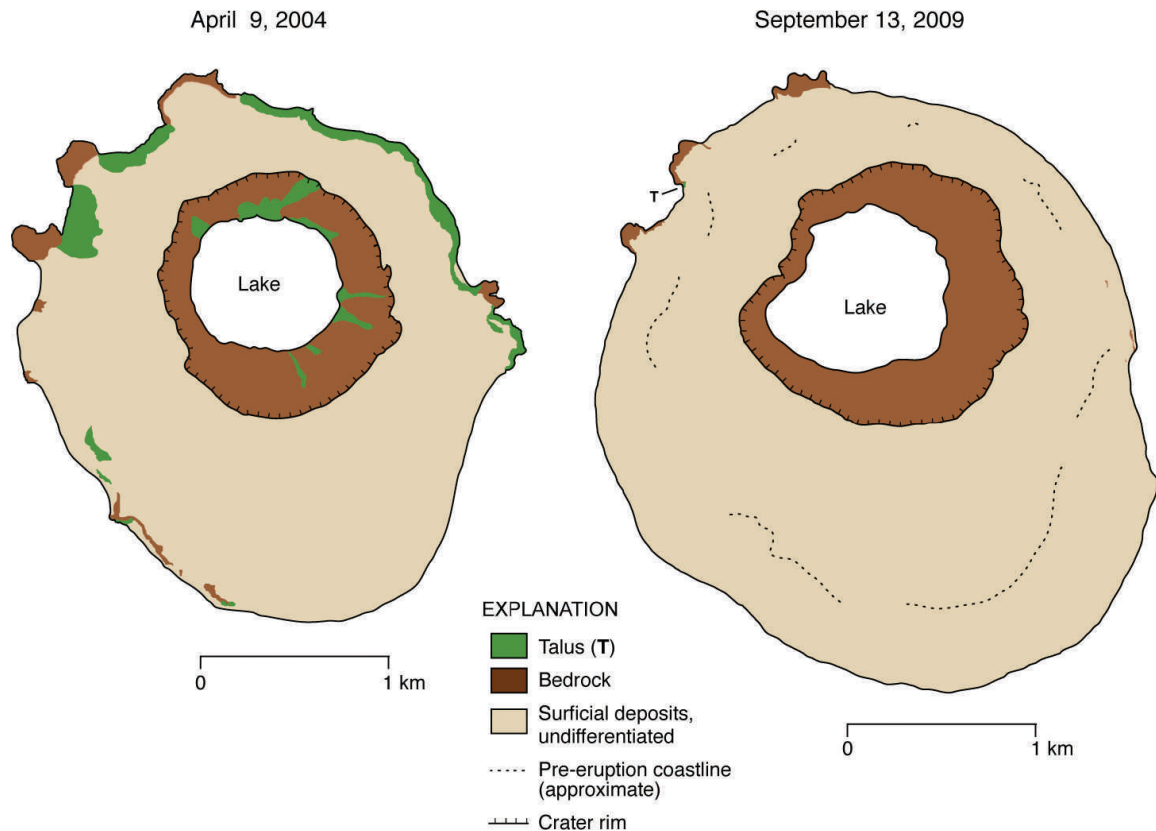


FIGURE 12. Maps of Kasatochi Island showing the extent of talus and bedrock on 9 April 2004, prior to the 2008 eruption and 13 September 2009, about one year after the eruption. Areas of talus on the island are important nesting habitat for seabirds.

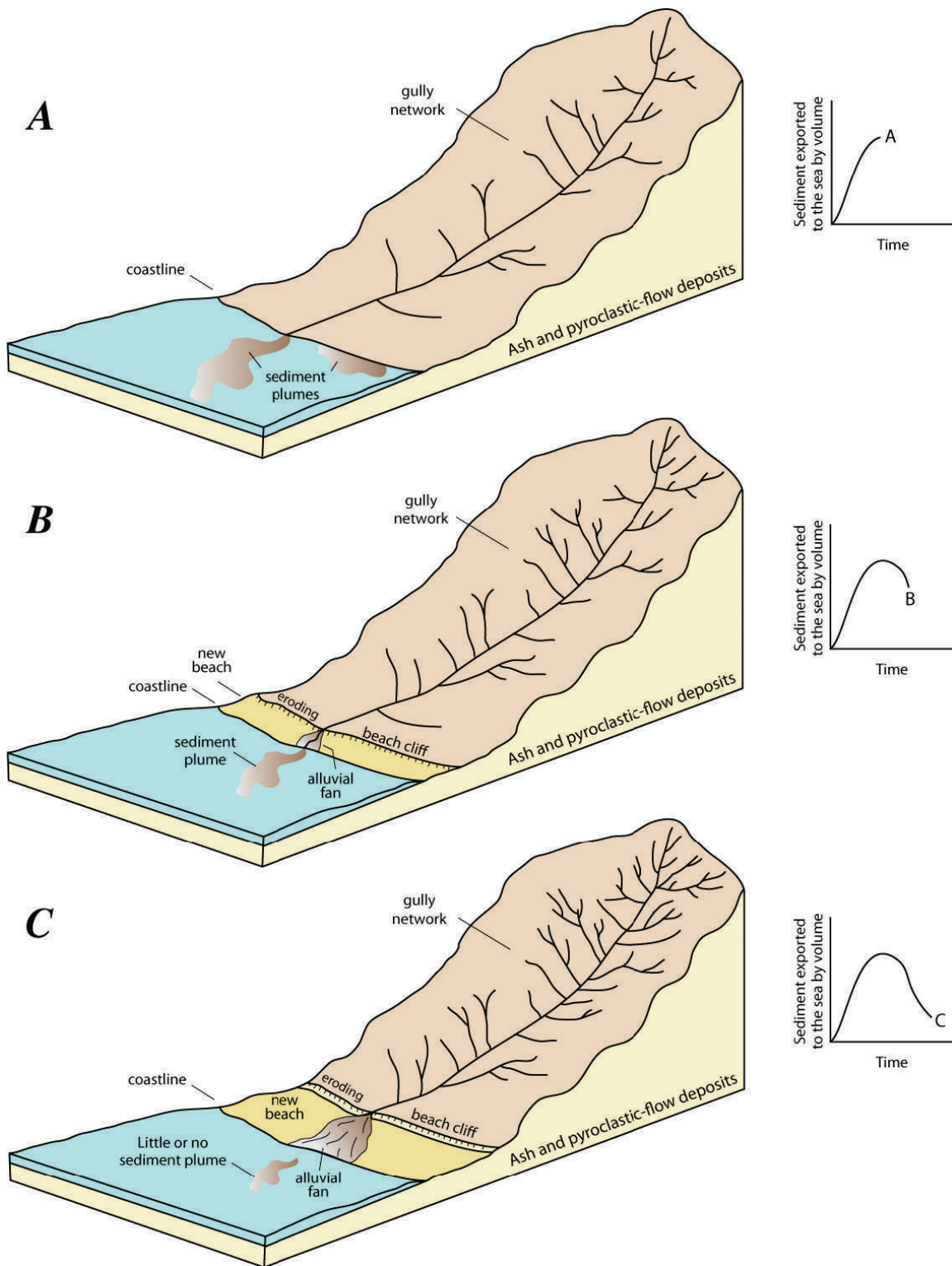
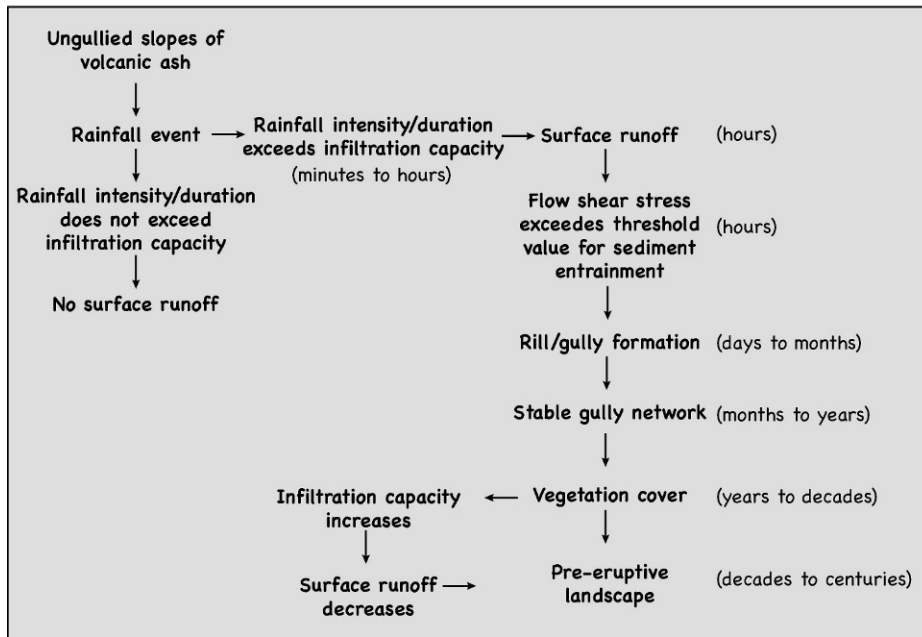


FIGURE 13. Schematic diagram illustrating the evolution of the gully network on the flanks of Kasatochi volcano and the interplay among sediment delivery to the coast and growth of new beaches. (A) Initial phase of gully development and approximate time of maximum sediment yield. (B) Intermediate phase of gully development and growth of new beaches. (C) Declining phase of gully growth and sediment yield. See text for further discussion.

area) amounts of rainfall may occur at any time. Although the climate of the area is maritime and wet, and the island is exposed to storms from all directions, rainfall intensity and duration for the region is typically low and large volumes of runoff are generally not generated. The ash-covered slopes of the volcano will

likely remain bare and unvegetated for some time, perhaps a decade or more. As a stable drainage network becomes established, it will require greater and greater amounts of runoff to erode and transport sediment to the sea. Thus, the impacts of elevated amounts of suspended sediment in the nearshore

Drainage Network



Coastal Erosion

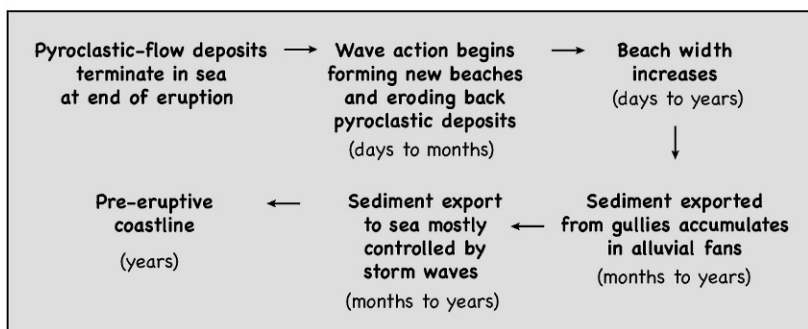


FIGURE 14. Summary of processes responsible for introducing sediment from Kasatochi Island into the sea.

environment around Kasatochi Island are likely to become more episodic and positively correlated with large storms.

As the gully system on Kasatochi Island begins to stabilize and sediment yield declines accordingly, wave action will remain the dominant, if not the only process for introducing sediment into the sea. Major storms and high surf are expected to be associated with periods of high rates of coastal erosion and nearshore sediment dispersal and thus the ecological impact of elevated suspended sediment loads in the sea will be episodic and likely of relatively short duration.

TABLE 5

Major physiographic changes of Kasatochi Island resulting from the 7–8 August 2008 eruption.

	9 April 2004 (pre-eruption)	17 Sept. 2008 (post-eruption)	Percent change
Island area (km ²)	5.0	7	40
Island perimeter (km)	10.2	10.4	2
Crater area (km ²)	1.2	1.5*	25
Lake area (km ²)	0.4	0.7*	73

* Data from 18 April 2009 Quickbird image.

Acknowledgments

Funding for this work was provided by a grant from the North Pacific Research Board, Project #923, and the U.S. Geological Survey Volcano Hazards Program. The authors thank the crew and staff of the U.S. Fish and Wildlife Service R/V *Tiglax* for logistical support of our work on Kasatochi Island. Review comments by two anonymous reviewers and the associate editor are appreciated and helped improve the clarity of the manuscript. This is contribution 253 of the North Pacific Research Board.

TABLE 6

Coastline erosion estimates.

Sector	Average erosion rate		
	8 Aug.– 17 Sept. 2008 (meters per day)	17 Sept. 2008– 18 April 2009 (meters per day)	18 April– 13 Sept. 2009 (meters per day)
NW	0.9	0.26	0.22
NE	0.88	0.37	0.26
SE	1.23	0.55	0.36
SW	0.89	0.52	0.39

References Cited

- Anderson, J. R., and Gyakum, J. R., 1989: A diagnostic study of Pacific Basin circulation regimes as determined from extra-tropical cyclone tracks. *Monthly Weather Review*, 117: 2672–2686.
- Bull, L. J., and Kirkby, M. J., 1997: Gully processes and modeling. *Progress in Physical Geography*, 21: 354–374.
- Casali, J., López, J. J., and Giráldez, J. V., 2003: A process-based model for channel degradation: application to ephemeral gully erosion. *Catena*, 50: 435–447.
- Chinen, T., and Kadomura, H., 1986: Post-eruption sediment budget of a small catchment on Mt. Usu, Hokkaido. *Zeitschrift für Geomorphologie*, 60: 217–232.
- Collins, B. D., and Dunne, T., 1986: Erosion of tephra from the 1980 eruption of Mount St. Helens. *Geological Society of America Bulletin*, 97: 896–905.
- Collins, D. B. G., and Bras, R. L., 2004: Modeling the effects of vegetation-erosion coupling on landscape evolution. *Journal of Geophysical Research*, 109: article F03004, doi:10.1029/2003JF000028.
- Dale, V. H., Swanson, F. J., and Crisafulli, C. M. (eds.), 2005: *Ecological Responses to the Eruption of Mount St. Helens*. New York: Springer.
- Engdahl, E. R., Billington, S., and Kisslinger, C., 1989: Teleseismically recorded seismicity before and after the May 7, 1986, Andreanof Islands, Alaska, earthquake. *Journal of Geophysical Research*, 94: 15481–15498.
- Erskine, W., 2005: Gully erosion. In Lehr, J., and Keeley, J. (eds.), *Water Encyclopedia: Surface and Agricultural Water*. Hoboken: Wiley-Interscience, 183–188.
- Favis-Mortlock, D. T., Guerra, A. J. T., and Boardman, J., 1998: A self-organizing dynamic systems approach to hillslope rill initiation and growth: model development and validation. In Summer, W., Klaghofer, E., and Zhang, W. (eds.), *Modeling Soil Erosion, Sediment Transport and Closely Related Hydrological Processes*. Wallingford: IAHS, International Association of Hydrological Sciences Publication, 249: 53–61.
- Flanagan, D. C., Ascough, J. C., Nearing, M. A., and Laflen, J. M., 2001: The water erosion prediction project (WEPP) model. In Harmon, R. S., and Doe, W. W. (eds.), *Landscape Erosion and Evolution Modeling*. New York: Kluwer Academic, 145–199.
- Gran, K. B., and Montgomery, D. R., 2005: Spatial and temporal patterns in fluvial recovery following volcanic eruptions: channel response to basin-wide sediment loading at Mount Pinatubo, Philippines. *Geological Society of America Bulletin*, 117: 195–211.
- Hairsine, P. B., and Rose, C. W., 1992a: Modeling water erosion due to overland flow using physical principles: 1. Sheet flow. *Water Resources Research*, 28: 237–243.
- Hairsine, P. B., and Rose, C. W., 1992b: Modeling water erosion due to overland flow using physical principles: 2. Rill flow. *Water Resources Research*, 28: 245–250.
- Hayes, S. K., Montgomery, D. R., and Newhall, C. G., 2002: Fluvial sediment transport and deposition following the 1991 eruption of Mount Pinatubo. *Geomorphology*, 45: 211–224.
- Horton, R. E., 1945: Erosional development of streams and their drainage basins; hydrophysical approach to quantitative morphology. *Geological Society of America Bulletin*, 56: 275–370.
- Istanbulluoglu, E., and Bras, R. L., 2005: Vegetation-modulated landscape evolution: effects of vegetation on landscape processes, drainage density, and topography. *Journal of Geophysical Research*, 110: article F02012, doi:10.1029/2004JF000249.
- Janda, R. J., Daag, A. S., Delos Reyes, P. J., Newhall, C. G., Pierson, T. C., Punongbayan, R. S., Rodolfo, K. S., Solidum, R. U., and Umbal, J. V., 1996: Assessment and response to lahar hazard around Mount Pinatubo, 1991 to 1993. In Newhall, C. G., and Punongbayan, R. S. (eds.), *Fire and Mud: Eruptions and Lahars of Mount Pinatubo*. Quezon City, Philippines: Philippine Institute of Volcanology and Seismology, and Seattle: University of Washington Press, 107–137.
- Jewett, S. C., Bodkin, J. L., Chenelot, H., Esslinger, G. G., and Hoberg, M. K., 2010: The nearshore benthic community of Kasatochi Island, one year after the 2008 volcanic eruption. *Arctic, Antarctic, and Alpine Research*, 42: 315–324.
- Karagulian, F., Clarisse, L., Clerbaux, C., Prata, A. J., Hurtmans, D., and Coheur, P. F., 2010: Detection of volcanic SO₂, ash, and H₂SO₄ using the Infrared Atmospheric Sounding Interferometer (IASI). *Journal of Geophysical Research*, 115: article D00L02, doi:10.1029/2009JD012786.
- Kirkby, M. J., and Bracken, L. J., 2009: Gully processes and gully dynamics. *Earth Surface Processes and Landforms*, 34: 1841–1851.
- Kuenzi, W. D., Horst, O. H., and McGehee., 1979: Effect of volcanic activity of fluvial-deltaic sedimentation in a modern arc-trench gap, southwestern Guatemala. *Geological Society of America Bulletin*, 90: 827–838.
- Lander, J., 1996: Tsunamis affecting Alaska, 1737–1996. Boulder, Colorado: U.S. Department of Commerce, National Oceanic and Atmospheric Administration, National Environmental Satellite Data and Information Service, National Geophysical Data Center, 195 pp.
- Lavigne, F., 2004: Rate of sediment yield following small-scale volcanic eruptions: a quantitative assessment at Merapi and Semeru stratovolcanoes, Java, Indonesia. *Earth Surface Processes and Landforms*, 29: 1045–1058.
- Leavesley, G. H., Lusby, G. C., and Lichty, R. W., 1989: Infiltration and erosion characteristics of selected tephra deposits from the 1980 eruption of Mount St. Helens, Washington, USA. *Hydrological Sciences Journal*, 34: 339–353.
- Major, J. J., 2004: Posteruption suspended sediment transport at Mount St. Helens: decadal-scale relationships with landscape adjustments and river discharges. *Journal of Geophysical Research*, 109: article F01002, doi:10.1029/2002JF000010.
- Major, J. J., and Mark, L. E., 2006: Peak flow responses to landscape disturbances caused by the cataclysmic 1980 eruption of Mount St. Helens, Washington. *Geological Society of America Bulletin*, 118: 938–958.
- Major, J. J., and Yamakoshi, T., 2005: Decadal-scale change of infiltration characteristics of a tephra-mantled hillslope at Mount St. Helens, Washington. *Hydrological Processes*, 19: 3621–3630.
- Major, J. J., Pierson, T. C., Dinehart, R. L., and Costa, J. E., 2000: Sediment yield following severe volcanic disturbance—A two decade perspective from Mount St. Helens. *Geology*, 28: 819–822.
- Manville, V., Németh, K., and Kano, K., 2009: Source to sink: a review of three decades of progress in the understanding of volcanoclastic processes, deposits, and hazards. *Sedimentary Geology*, 220: 136–161.
- Milliman, J. D., and Syvitski, J. P. M., 1992: Geomorphic/tectonic control of sediment discharge to the ocean: the importance of small mountainous rivers. *Journal of Geology*, 100: 525–544.
- Montgomery, D. R., and Dietrich, W. E., 1989: Source areas, drainage density, and channel initiation. *Water Resources Research*, 25: 1907–1918.
- Overland, J. E., Adams, J. M., and Bond, N. A., 1999: Decadal variability of the Aleutian Low and its relation to high-latitude circulation. *Journal of Climate*, 12: 1542–1548.
- Rodionov, S. N., Overland, J. E., and Bond, N. A., 2005: Spatial and temporal variability of the Aleutian climate. *Fisheries Oceanography*, 14: 3–21.
- Rodionov, S. N., Bond, N. A., and Overland, J. E., 2007: The Aleutian Low, storm tracks, and winter climate variability in the Bering Sea. *Deep-Sea Research II*, 53: 2560–2577.
- Rosenfeld, C., 1987: Observation and measurement of erosion following the 1980 eruptions of Mount St. Helens, Washington,

- USA. In Godard, A., and Rapp, A. (eds.), *Processus et mesure de l'érosion*, 25th International Geographical Congress, CNRS Paris, 565–571.
- Ryan, H. F., and Scholl, D. W., 1989: Geologic implications of great intraplate earthquakes along the Aleutian arc. *Journal of Geophysical Research*, 98: 135–146.
- Schumm, S. A., and Rea, D. K., 1995: Sediment yield from disturbed Earth systems. *Geology*, 23: 391–394.
- Scott, W. E., Nye, C. J., Waythomas, C. F., and Neal, C. A., 2010: August 2008 eruption of Kasatochi volcano, Aleutian Islands, Alaska—Resetting an island landscape, *Arctic, Antarctic, and Alpine Research*, 42: 250–259.
- Segerstrom, K., 1960: Erosion and related phenomena at Paricutin in 1957. *U.S. Geological Survey Bulletin*, 1104-A: 18 pp.
- Segerstrom, K., 1966: Paricutin, 1965—Aftermath of eruption. *U.S. Geological Survey Professional Paper*, 550-C: C93–C101.
- Shimokawa, E., and Jitousono, T., 1987: Rate of erosion on tephra-covered slopes of volcanoes. *Transactions, Japanese Geomorphological Union*, 8: 269–286.
- Shimokawa, E., and Taniguchi, Y., 1983: Sediment yield from hillslopes on active volcanoes. In *Proceedings of Symposium on Erosion Control in Volcanic Areas*. Tokyo: Japan Public Works Research Institute, Ministry of Construction, Technical Memorandum 1908, 155–182.
- Shimokawa, E., Jitousono, T., and Tsuchiya, S., 1996: Sediment yield from the 1984 pyroclastic-flow deposit covered hillslopes in Merapi Volcano, Indonesia. *Journal of the Japan Society of Erosion Control Engineering*, 48: 101–108.
- Sidorchuck, A., 1999: Dynamic and static models of gully erosion. *Catena*, 37: 401–414.
- Suwa, H., and Yamakashi, T., 1999: Sediment discharge by storm runoff at volcanic torrents affected by eruption. *Zeitschrift für Geomorphologie*, 114: 6–88.
- Swanson, F. J., and Major, J. J., 2005: Physical environments, events, and geological-ecological interactions at Mount St. Helens—March 1980–2004. In Dale, V. H., Swanson, F. J., and Crisafulli, C. M. (eds.), *Ecological Responses to the 1980 Eruption of Mount St. Helens*. New York: Springer-Verlag, 27–44.
- Swanson, R. J., Collins, B., Dunne, T., and Wichersky, B. P., 1983: Erosion of hillslopes affected by volcanic eruption. In *Proceedings of Symposium on Erosion Control in Volcanic Areas*. Tokyo: Japan Public Works Research Institute, Ministry of Construction, Technical Memorandum 1908, 183–222.
- Sykes, L. R., 1971: Aftershock zones of great earthquakes, seismicity gaps, and earthquake prediction for Alaska and the Aleutians. *Journal of Geophysical Research*, 76: 8021–8041.
- Talbot, S. S., Talbot, S. L., and Walker, L. R., 2010: Post-eruption legacy effects and their implications for long-term recovery of the vegetation on Kasatochi Island, Alaska. *Arctic, Antarctic, and Alpine Research*, 42: 285–296.
- Trenberth, K. E., 1990: Recent observed interdecadal climate changes in the northern hemisphere. *Bulletin of the American Meteorological Society*, 71: 988–993.
- Walling, D. E., and Webb, B. W., 1996: Erosion and sediment yield: a global overview. *International Association of Hydrological Science Publication*, 236: 3–19.
- Waythomas, C. F., and Williams, G. P., 1988: Sediment yield and spurious correlation—Towards a better portrayal of the annual suspended-sediment load of rivers. *Geomorphology*, 1: 309–316.
- Waythomas, C. F., Scott, W. E., Prejean, S. G., Schneider, D. J., Izbekov, P., and Nye, C. J., 2010: The August 7–8, 2008 eruption of Kasatochi volcano, central Aleutian Islands, Alaska. *Journal of Geophysical Research*, in review.
- Williams, J. C., Drummond, B. A., and Buxton, R. T., 2010: Initial effects of the August 2008 volcanic eruption on breeding birds and marine mammals at Kasatochi Island, Alaska. *Arctic, Antarctic, and Alpine Research*, 42: 306–314.
- Wischmeier, W. H., and Smith, D. D., 1978: Predicting rainfall erosion losses. Washington, D.C.: USDA, *USDA Agricultural Research Services Handbook*, 537: 57 pp.
- Yamamoto, H., 1984: Erosion of the 1977–1978 tephra layers on a slope of Usu Volcano, Hokkaido. *Transactions, Japanese Geomorphological Union*, 5: 111–124.

MS accepted June 2010